

Characterizing Deprived Urban Areas Using Remote Sensing

1st Yvette Espinoza
Software Engineer
Northrop Grumman
Redondo Beach, CA, USA
yespinoz@purdue.edu

Abstract—The urban population has increased dramatically in the last few decades, but the rapid rate of urbanization has caused a strain on the available resources, leaving many to live in deprived, or impoverished areas. To address these socio-demographic issues policymakers typically rely on traditional survey-based data, like the census, but such data is complex to acquire and can quickly become outdated. Earth observations are the proposed solution to the gaps left by traditional data. Artificial intelligence and deep learning algorithms are being used to detect changes on the earth’s surface, such as detecting new urban areas. New research has focused on classifying elements of the city itself, monitoring waste disposal sites and traffic to have a better understanding of the deprived areas and their needs. This project will analyze urban characteristics, what makes an area ‘deprived’, and discuss the uses of remote sensing in socio-demographic applications by collecting and preprocessing SAR data that would be used for classification.

I. LITERATURE REVIEW

It is estimated that half of the world’s population is currently living in cities, with that number expected to rise to 60% by 2030, but the rapid rate of urbanization has not resulted in an equal increase in public amenities or affordable housing [2]. The lack of affordable housing has led to the creation of informal settlements, commonly referred to as ‘slums’, or deprived urban areas (DUA). These areas of concentrated poverty often lack public amenities such as access to clean water or waste disposal, and are known to have hazardous effects on the inhabitants health [4].

Poverty reduction, listed in the United Nation’s Sustainable Development Goals, is a priority worldwide, though policies enacted and definition of poverty itself vary between countries. Some common definitions include the current financial status of residents, or the value of a household’s assets, but such methods alone do not paint a clear picture of the situation, since low income households do not necessarily belong to a deprived area [11]. Since research has found poverty is related to population growth, one reduction approach focuses on addressing deprived urban areas, thus improving living conditions and reducing the risk of natural hazards [10].

The traditional methods for mapping deprived areas rely on field surveys, such as the census, however these methods are costly and have a long period between collections. Since settlements are constantly changing, the data quickly becomes outdated and unable to provide feedback on whether any policies are effective [15]. The COVID-19 pandemic brought

more attention to this problem when many field surveys were delayed during a time when data was needed to divert resources to the most affected communities. One solution to fill the data gaps left by the traditional methods is to use remote sensing.

A. Remote Sensing

There are many ways in which remote sensing can be used to get a better understanding of an area. At a high level, satellite images can be used to train deep learning models that classify areas as urban or rural [5], but research has also focused on smaller features, such as waste piles and vehicles.

Radar systems are desirable for data collection because they are not affected by weather conditions such as clouds or lighting. The X band of Synthetic Aperture Radars (SAR), which has frequencies in the range of 8-12 GHz, produces high resolution images that can be analyzed for feature extraction [16]. The C band, operating from 4-8 GHz, though not as high resolution as the X band, can penetrate deeper, making it a good option for classifying landscapes [6]. A disadvantage to SAR is the lack of large datasets that can be used for training the models that extract features from urban areas [12], but its independence of atmospheric conditions and cloud cover make it a more reliable source of data.

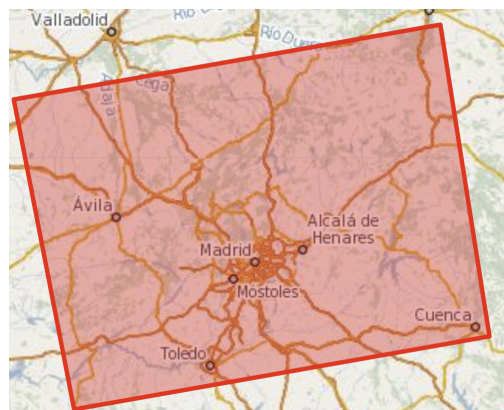


Fig. 1. The region of interest from the Sentinel-1 data acquired on April 2, 2022.

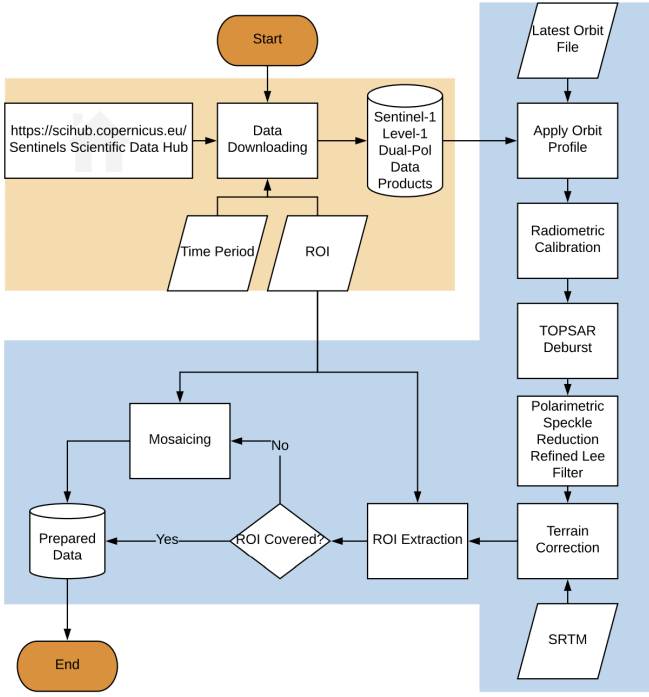


Fig. 2. Sentinel-1 data processing flowchart, provided by [6]. The orange area is the data collection and the blue area is the data processing done in SNAP.

B. Polarimetry

Dual polarization, where a signal is transmitted in one polarization and received in both polarization's, either HH/HV or VV/VH, is used to provide additional surface details.

C. Texture Analysis

Texture analysis, characterizing an image by its texture content, is commonly used in remote sensing because of its effectiveness in classification [7]. One form of texture analysis uses the gray level co-occurrence matrix (GLCM) which contains a mapping of how often a pixel with intensity i appears alongside a pixel of intensity j . The GLCM can be used to extract 14 texture statistics, with the most commonly used shown in Table I where P_{ij} is the (i,j) entry in the matrix. Due to the large size of the SAR data collected from missions like Sentinel-1, the GLCM is more efficiently extracted using tools developed specifically for processing SAR data, like SNAP, explained at a later section.

Of the texture statistics, variance has the best performance when differentiating between DUA's and formal areas, since a high variance gives a sharp change in the pixels that usually denote building edges or a drastic change in the environment [9]. The other statistics also provide valuable information, with contrast used to map DUA expansions and entropy as a validation step, since DUA's naturally have high entropy [8].

D. Individual Contribution

For the individual contribution the data collection and processing from [6] will be implemented. Sentinel-1 dual-pol

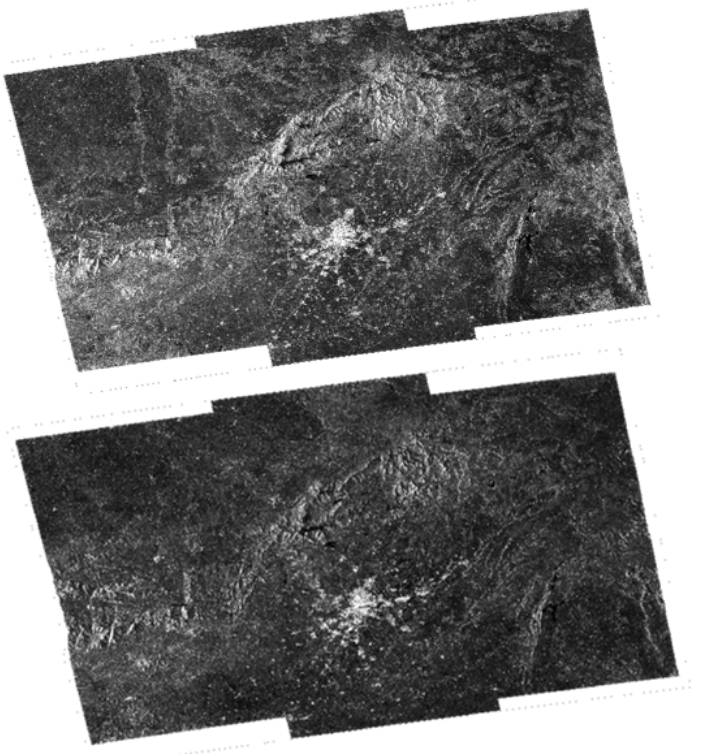


Fig. 3. The intensity images generated after preprocessing the data. The top image is for VH and the bottom for VV polarization's.

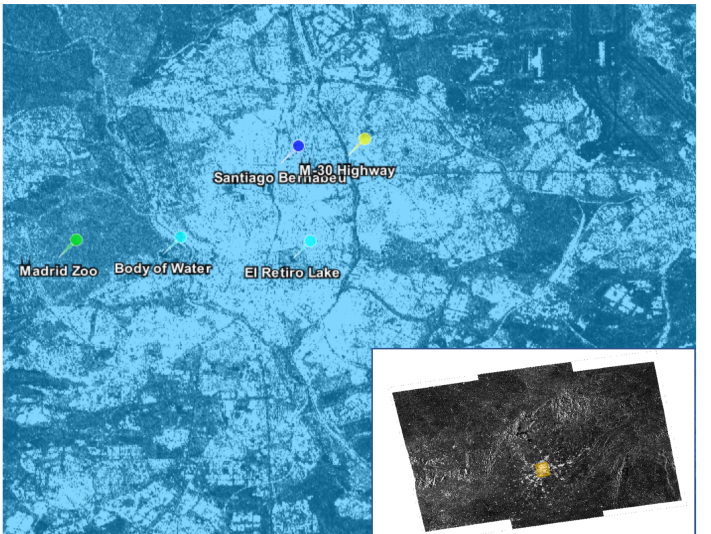


Fig. 4. The VV polarization image was annotated with pins to show El Retiro Lake (40.417° N, 3.683° W) and the Santiago Bernabeu Stadium (40.452° N, 3.688° W). Three other pins were added to show more general areas, the Madrid Zoo for grassland, the M-30 highway, and a body of water.

TABLE I
COMMON GLCM STATISTICS

Statistic	Formula
Energy	$\sum_{i,j=0}^{N-1} P_{ij}^2$
Contrast	$\sum_{i,j=0}^{N-1} P_{ij}(i - j)^2$
Entropy	$\sum_{i,j=0}^{N-1} P_{ij}(-\ln(P_{ij}))$
Variance	$\sigma_i = \sum_{i=0}^{N-1} P_{ij}(i - \mu_i)^2$
Homogeneity	$\sum_{i,j=0}^{N-1} (P_{ij}/1 + (i - j)^2)$

SAR data (VV/VH) will be collected, then processed to obtain the GLCM and texture statistics.

II. DATA COLLECTION AND PROCESSING

The dual-pol data was collected by Sentinel-1 and accessed via the Copernicus Open Access Hub (<https://scihub.copernicus.eu>) which has free and open access to the Sentinel missions. There are four acquisition modes to chose from on Sentinel-1: Stripmap (SM), Interferometric Wide swath (IW), Extra-Wide swath (EW) and Wave (WV). The WV acquisition mode was considered unfit for the project because it only contained single polarization when dual polarization was needed [1]. For the remaining three acquisition modes, there are two products to choose from: Single Look Complex (SLC) and Ground Range Detected (GRD). One difference between the two products is that SLC contains phase information, which is not included in the GRD product.

In [16] the SM mode was used, though no explanation was provided for that choice, while [6] used the SLC product from the IW acquisition mode because of the phase information that was needed for classification. The data processing steps are shown in Figure 2, provided by [6].

A. Sentinel Application Platform

The Sentinel Application Platform (SNAP) is an open access graphical user interface created to process SAR data from various missions, including Sentinel.

a) *Calibration*: Before the SAR data can be used it must first be calibrated. Sentinel data comes with calibration files that are used by SNAP to correctly represent the radar backscatter of the reflecting surface. If the phase information is needed, the calibration output should be saved as a complex value.

b) *TOPSAR Deburst*: The IW acquisition mode captures three swath's per polarization, resulting in six images for dual-pol data. The TOPSAR Deburst is used to merge the six images into one image.

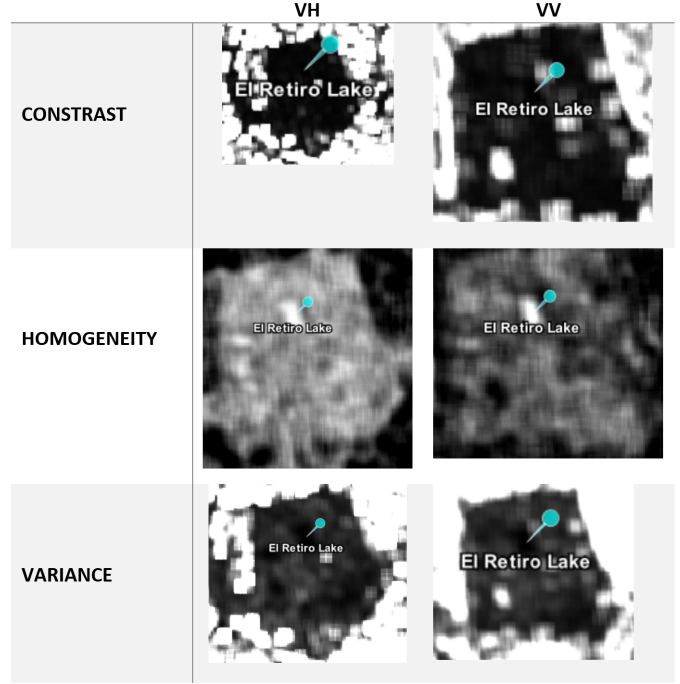


Fig. 5. The textures corresponding to the area around El Retiro Lake. The homogeneity values were higher for the lake, displayed as white, making it the only texture statistic that could differentiate water from its surroundings.

c) *Speckle Reduction*: SAR images come with speckle noise, generated by the interference of reflected waves [3], which reduces the quality of the images. Speckle noise filters are used to reduce the noise, but a careful balance is needed, since removing speckle also results in loss of detailed information [17]. The refined Lee filter, available in SNAP, is a popular filter because of its superior performance in preserving edges, linear features, and texture information [3].

d) *Terrain Correction*: Terrain correction is needed to correct the geometric distortions in the image by converting the slant range into a coordinate system of choice.

III. RESULTS

The time period and region of interest were chosen arbitrarily. The acquired data was from April 2, 2022 6:11 PM, which happened to capture Madrid, Spain. The region is shown in Figure 1. The output after data processing is shown in Figure 3.

Though the generated images are not as high resolution as multispectral images would be, they are still able to differentiate important landmarks, like the outlines of an urban area. Figure 4 shows the city of Madrid annotated with 5 pins to show distinct features. Two pins depict water, a large body of water near the zoo and El Retiro Lake, which is surrounded by gardens, one pin was added on El Santiago Bernabeu Stadium to depict a dense urban area, another was added on the Madrid Zoo, and the last was on the M-30 highway. The bottom right of the annotated image shows a yellow square around this

focused are, showing how the city of Madrid was just a tiny portion of the overall data collected.

TABLE II
GLCM STATISTICS FOR THE PIXELS CORRESPONDING TO THE 5 PINS:
TOP FOR VH, BOTTOM FOR VV

Pin/Feature	Contrast	Energy	Variance	Homogeneity
El Retiro Lake	0	2	2	2
Santiago Bernabeu	58.7	0.429	65.85	0.739
Body of Water	0	2	2	2
Madrid Zoo	1.086	1.01	4.871	1.457
M-30 Highway	0.086	1.915	2.128	1.95
El Retiro Lake	0.557	1.482	2.878	1.721
Santiago Bernabeu	401.28	0.206	885.58	0.19
Body of Water	0.086	1.915	2.129	1.957
Madrid Zoo	4.142	0.656	33.214	1.101
M-30 Highway	447.386	0.217	530.93	0.3213

For the texture analysis, SNAP was used to extract the following: contrast, homogeneity, energy, variance, and correlation. Due to the large size of the original data, a subset was created for the same area shown in Figure 4, on which the GLCM statistics were calculated. Table II shows the values for each statistic calculated on the pixel associated with the 5 pins on the map.

Previous studies [18] found homogeneity was best at detecting bodies of water. Figure 5 shows the texture statistics around El Retiro Lake, in which homogeneity was the only one able to differentiate the lake from the surrounding park. The homogeneity values for the 2 bodies of water also had the highest values compared to the other landmarks observed.

Variance is used to differentiate formal urban areas from deprived areas. The Santiago Bernabeu is located in a dense part of the city, which would be considered a formal urban area, confirming the designation as it scored the highest values for variance.

All processing was done in SNAP, but since the end product was about 150 GB, only the original data was uploaded to Github where the project is archived: <https://github.com/Yvette4/AAE523>

IV. CONCLUSION

The results from the GLCM statistics confirmed what other studies had found. The homogeneity was the best for detecting bodies of water, while the variance was best at detecting formal urban areas. One problem with the analysis is that Madrid, Spain does not have much variation in its urban landscape, so no information was collected on informal settlements or deprived urban areas.

Another complication with the project was the Sentinel-1 SNAP toolbox, which is a very complex and resource intense program. The first steps of preprocessing, orbit file and calibration, took longer than anticipated because of memory constraints which required modifying the default settings before the calculations could run. There are many other features,

like a feature to extract urban areas, that do not have much documentation but often came up in the help forums. The Sentinel-1 toolbox also has PCA and classification tools, though there was not enough time to investigate these. Future work on this project would require a better understanding of the tools to take full advantage of all there is to offer.

Overall the project was a meaningful way to understand SAR data, how to process it and interpret the findings with respect to urban area characteristics.

REFERENCES

- [1] *Acquisition Modes*. URL: <https://sentinels.copernicus.eu/web/sentinel/user-guides/sentinel-1-sar/acquisition-modes>.
- [2] UN. Department of Economic and Social Affairs. *The Sustainable development goals report 2019*. 2019. URL: <https://digitallibrary.un.org/record/3812145>.
- [3] Federico Filippioni. “Sentinel-1 GRD Preprocessing Workflow”. In: *Proceedings* 18.1 (2019). ISSN: 2504-3900. DOI: 10.3390/ECRS-3-06201. URL: <https://www.mdpi.com/2504-3900/18/1/11>.
- [4] Stefanos Georganos et al. “Is It All the Same? Mapping and Characterizing Deprived Urban Areas Using WorldView-3 Superspectral Imagery. A Case Study in Nairobi, Kenya”. In: *Remote Sensing* 13.24 (2021). ISSN: 2072-4292. DOI: 10.3390/rs13244986. URL: <https://www.mdpi.com/2072-4292/13/24/4986>.
- [5] Jinxin Guo et al. “Identify Urban Area From Remote Sensing Image Using Deep Learning Method”. In: *IGARSS 2019 - 2019 IEEE International Geoscience and Remote Sensing Symposium*. 2019, pp. 7407–7410. DOI: 10.1109/IGARSS.2019.8898874.
- [6] Jingliang Hu, Pedram Ghamisi, and Xiao Xiang Zhu. “Feature Extraction and Selection of Sentinel-1 Dual-Pol Data for Global-Scale Local Climate Zone Classification”. In: *ISPRS International Journal of Geo-Information* 7.9 (2018). ISSN: 2220-9964. DOI: 10.3390/ijgi7090379. URL: <https://www.mdpi.com/2220-9964/7/9/379>.
- [7] Xin Huang, Xiaobo Liu, and Liangpei Zhang. “A Multichannel Gray Level Co-Occurrence Matrix for Multi/Hyperspectral Image Texture Representation”. In: *Remote Sensing* 6.9 (2014), pp. 8424–8445. ISSN: 2072-4292. DOI: 10.3390/rs6098424. URL: <https://www.mdpi.com/2072-4292/6/9/8424>.
- [8] Monika Kuffer et al. “Extraction of Slum Areas From VHR Imagery Using GLCM Variance”. In: *IEEE Journal of Selected Topics in Applied Earth Observations and Remote Sensing* 9.5 (2016), pp. 1830–1840. DOI: 10.1109/JSTARS.2016.2538563.
- [9] Monika Kuffer et al. “The utility of the co-occurrence matrix to extract slum areas from VHR imagery”. In: *2015 Joint Urban Remote Sensing Event (JURSE)*. 2015, pp. 1–4. DOI: 10.1109/JURSE.2015.7120514.

- [10] Li Lin et al. “Remote Sensing of Urban Poverty and Gentrification”. In: *Remote Sensing* 13.20 (2021). ISSN: 2072-4292. DOI: 10.3390/rs13204022. URL: <https://www.mdpi.com/2072-4292/13/20/4022>.
- [11] Paloma Merodio Gómez et al. “Earth Observations and Statistics: Unlocking Sociodemographic Knowledge through the Power of Satellite Images”. In: *Sustainability* 13.22 (2021). ISSN: 2071-1050. DOI: 10.3390/su132212640. URL: <https://www.mdpi.com/2071-1050/13/22/12640>.
- [12] Wenzhong Shi et al. “Change Detection Based on Artificial Intelligence: State-of-the-Art and Challenges”. In: *Remote Sensing* 12.10 (2020). ISSN: 2072-4292. DOI: 10.3390/rs12101688. URL: <https://www.mdpi.com/2072-4292/12/10/1688>.
- [13] Dana Thomson et al. “Extending Data for Urban Health Decision-Making: a Menu of New and Potential Neighborhood-Level Health Determinants Datasets in LMICs”. In: *Journal of Urban Health* 96 (June 2019). DOI: 10.1007/s11524-019-00363-3.
- [14] Sabine Vanhuyse et al. “Gridded Urban Deprivation Probability from Open Optical Imagery and Dual-Pol Sar Data”. In: *2021 IEEE International Geoscience and Remote Sensing Symposium IGARSS*. 2021, pp. 2110–2113. DOI: 10.1109/IGARSS47720.2021.9554231.
- [15] Trecia Kay-Ann Williams, Tao Wei, and Xiaolin Zhu. “Mapping Urban Slum Settlements Using Very High-Resolution Imagery and Land Boundary Data”. In: *IEEE Journal of Selected Topics in Applied Earth Observations and Remote Sensing* 13 (2020), pp. 166–177. DOI: 10.1109/JSTARS.2019.2954407.
- [16] Michael Wurm et al. “Slum mapping in polarimetric SAR data using spatial features”. In: *Remote Sensing of Environment* 194 (2017), pp. 190–204. ISSN: 0034-4257. DOI: <https://doi.org/10.1016/j.rse.2017.03.030>. URL: <https://www.sciencedirect.com/science/article/pii/S0034425717301335>.
- [17] Aiyeola Sikiru Yommy et al. “SAR Image Despeckling Using Refined Lee Filter”. In: *2015 7th International Conference on Intelligent Human-Machine Systems and Cybernetics*. Vol. 2. 2015, pp. 260–265. DOI: 10.1109/IHMSC.2015.236.
- [18] Zhao Zheng, Zhang JiXian, and Huang Guo-man. “THE TEXTURAL ANALYSIS AND INTERPRETATION OF HIGH RESOLUTION AIRSAR IMAGES”. In: 2004.